Journal of Chemical Health Risks

www.jchr.org

JCHR (2025) 15(3), 2586-2592 | ISSN:2251-6727

Synthesis, Anticancer Activity and Molecular Docking of Quinazolinedione derivatives

Anjali Yadav, Anurag Singh, Shailesh Pathak, Dr. Arvind Kumar Srivastav

Shambhunath Institute of Pharmacy, Jhalwa,Prayagraj, U.P. India

(Received: 16 March 2025 Revised: 20 April 2025 Accepted: 15 June 2025)

KEYWORDS
Quinazolinidione derivatives, Anticancer activity, Molecular docking, MCF7

ABSTRACT:
A new series of quinazolinidione–amide derivatives (B1–B5) was synthesized through a two-step procedure involving palladium-catalyzed cyclization followed by amide coupling with substituted anilines. The structures of the synthesized compounds were confirmed using spectroscopic techniques such as ^{1}H NMR and LCMS, and their purity was validated through elemental analysis. The anticancer activity of the compounds was evaluated in vitro against the MCF-7 human breast cancer cell line using the Sulforhodamine B (SRB) assay. Among the tested derivatives, B3 and B5 exhibited significant cytotoxicity, with IC_{50} values of 9.1 µg/mL and 10.2 µg/mL, respectively, compared to standard drugs Doxorubicin and Erlotinib. Molecular docking studies were conducted using AutoDock Vina to predict protein–ligand interactions with the target receptor (PDB ID: 1M17). The results revealed strong binding affinities for all synthesized compounds, with B5 displaying the highest docking score (–9.9 kcal/mol). Consistent hydrophobic and hydrogen-bonding interactions were observed across the series. Overall, the integrated synthetic, biological, and computational findings suggest that compounds B3 and B5 are promising candidates for further development as anticancer agents.

INTRODUCTION

Cancer remains one of the leading causes of mortality worldwide, despite the availability of a wide range of chemotherapeutic agents used either as monotherapies or in combination regimens. The clinical efficacy of many existing treatments is often limited by factors such as tumor heterogeneity, drug resistance, and the inability to selectively target malignant cells without affecting healthy tissues. These challenges underscore the urgent need for novel, more effective anticancer agents with improved selectivity and reduced side effects.

Heterocyclic scaffolds continue to attract significant attention in medicinal chemistry due to their structural diversity and broad spectrum of biological activities. Among them, quinazolinidiones have emerged as a particularly promising class of compounds, exhibiting a wide array of pharmacological properties including antimicrobial, anti-inflammatory, antiviral, CNS-modulating, and notably, anticancer effects. The core quinazolinidione framework offers synthetic flexibility, enabling the development of diverse derivatives tailored for specific therapeutic targets.

Motivated by the therapeutic potential of this class, and as a continuation of our research on quinazoline-based pharmacophores, we synthesized a new series of quinazolinidione–amide hybrids (B1–B5). These novel derivatives were designed to explore their cytotoxic potential against MCF-7 human breast cancer cell lines. In addition to in vitro biological evaluation, in silico molecular docking studies were conducted to assess their binding interactions with key oncogenic targets. This integrated experimental and computational approach was employed to identify promising lead compounds for further development in anticancer drug discovery.

MATERIAL AND METHODS

Chemistry

Procedure for Quinazolinidione Cyclization (A)

Compound 1 and Compound 2 were introduced into a dry reaction vessel, followed by the addition of palladium catalyst $Pd_2(dba)_3$, the Xantphos ligand, and cesium carbonate (Cs_2CO_3) as a base. The mixture was dissolved in dioxane and heated at 100 °C to initiate the cyclization reaction, resulting in the formation of the quinazolinidione intermediate (A). After the reaction reached completion, the mixture was filtered through a Celite pad, and the filtrate was extracted with ethyl acetate (EtOAc). The organic phase was then concentrated under reduced pressure to obtain the crude

Journal of Chemical Health Risks

www.jchr.org

JCHR (2025) 15(3), 2586-2592 | ISSN:2251-6727

product, which was subsequently purified by column chromatography to yield the pure intermediate A.

Procedure of Amide Coupling (B1-B5)

The quinazolinidione intermediate (A) was subjected to amide coupling with a series of substituted anilines to synthesize final derivatives B1–B5. The coupling reaction was carried out in dichloromethane (DCM) at ambient temperature (25 °C) using T3P (propylphosphonic anhydride) as the activating reagent and triethylamine (TEA) as the base. The reaction mixture was stirred for 4 hours.

Progress of the reaction was monitored by thin-layer chromatography (TLC) using a Benzene:Methanol (9:1) solvent system and confirmed via mass spectrometry. Upon completion, the reaction mixture was quenched with water and extracted with ethyl acetate (EtOAc). The combined organic layers were dried, concentrated under reduced pressure, and the resulting crude products were purified by column chromatography. The purified compounds B1–B5 were characterized by TLC, melting point determination, and spectroscopic techniques including NMR and mass spectrometry. Elemental analysis was performed to confirm the purity and composition of the final products.

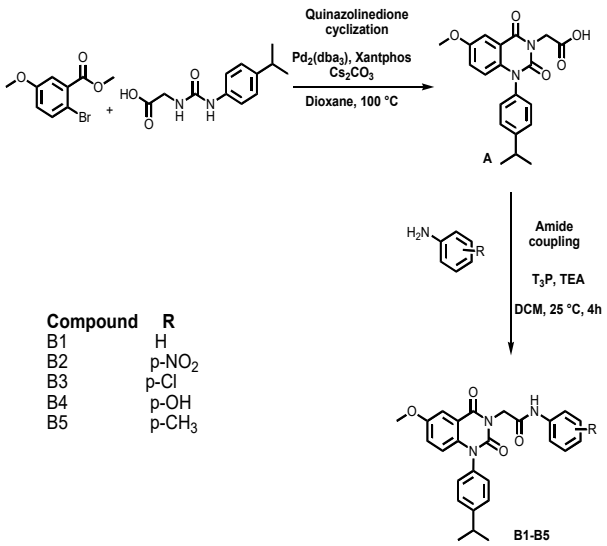

Table 1: Physico-Chemical data of compound B1-B5

Compound	Melting Point (°C)	Yield (%)	R_f
B1	186-188	66	0.58
B2	212-216	81	0.75
B3	174-176	84	0.79
B4	178-182	75	0.73
B5	202-206	86	0.73

Table 2: LCMS and 1H NMR of compound B1-B5

Compound	LCMS (m/z)	^{1}H NMR (ppm)
B1	443.18	1.29 (s, 3H), 1.35 (s, 3H), 2.85-3.24 (m, 1H), 3.85 (s, 3H), 4.19 (s, 1H), 5.94 (s, 1H), 7.09-8.49 (m, 13H)
B2	488.17	1.33 (s, 3H), 1.39 (s, 3H), 3.01-3.39 (m, 1H), 3.87 (s, 3H), 4.25 (s, 1H), 5.37 (s, 1H), 7.34-8.35 (m, 12H)
B3	477.15	1.30 (s, 3H), 1.37 (s, 3H), 2.86-3.25 (m, 1H), 3.85 (s, 3H), 4.28 (s, 1H), 5.63 (s, 1H), 7.15-8.35 (m, 12H)
B4	459.18	1.31 (s, 3H), 1.37 (s, 3H), 2.90â€“3.28 (m, 1H), 3.83 (s, 3H), 4.00 (s, 1H), 5.75 (s, 1H), 6.79â€–9.43 (m, 13H)
B5	457.2	1.25 (s, 3H), 1.32 (s, 3H), 2.32 (s, 1H), 2.81â€“3.20 (m, 1H), 3.74 (s, 3H), 4.11 (s, 1H), 5.08 (s, 1H), 7.10â€–8.92 (m, 12H)

Table 3: CHN analysis of compound B1-B5

Compound	Calculated			Experimental		
	C	H	N	C	H	N
B1	70.41	5.68	9.47	70.45	5.65	9.45
B2	63.93	4.95	11.47	63.91	4.92	11.43
B3	65.34	5.06	8.79	65.32	5.03	8.74
B4	67.96	5.48	9.14	67.93	5.45	9.12
B5	70.88	5.95	9.18	70.85	5.93	9.15

Journal of Chemical Health Risks

www.jchr.org

JCHR (2025) 15(3), 2586-2592 | ISSN:2251-6727

Biological Activity

***In vitro* anticancer activity (SRB Assay)**

The anticancer potential of the synthesized compounds B1–B5 was assessed using the Sulforhodamine B (SRB) colorimetric assay against the human breast cancer cell line MCF-7. Doxorubicin served as the standard reference compound for comparative analysis.

MCF-7 cells were cultured in RPMI-1640 or DMEM media, each supplemented with 10% fetal bovine serum (FBS), and maintained under standard incubation conditions (37 °C, 5% CO_2, humidified atmosphere). Cells were seeded into 96-well microplates at a density of 5×10^3 to 1×10^4 cells per well and allowed to adhere for 24 hours.

Post-incubation, cells were treated with varying concentrations (1, 10, 25, 50, and 100 µM) of test compounds, prepared in DMSO with a final DMSO concentration not exceeding 0.1%. Control wells received medium with 0.1% DMSO, while positive control wells were treated with either Doxorubicin or Erlotinib.

After 48 hours of exposure, the cells were fixed by the addition of 50 µL of ice-cold 50% trichloroacetic acid (TCA) and incubated at 4 °C for 1 hour. The plates were subsequently washed with tap water and air-dried. Each well was then stained with 100 µL of 0.4% SRB solution prepared in 1% acetic acid and incubated at room temperature for 30 minutes in the dark. Unbound dye was removed by rinsing with 1% acetic acid, and the plates were air-dried once again.

To solubilize the protein-bound SRB, 100 µL of 10 mM Tris base (pH 10.5) was added to each well, and the plates were gently agitated for 10 minutes. Absorbance was measured at 510 nm using a microplate reader.

Cell viability was calculated relative to the untreated control, and percentage growth inhibition was determined. IC_{50} values (concentration required to inhibit 50% of cell growth) were computed using nonlinear regression analysis in GraphPad Prism. All experiments were conducted in triplicate to ensure consistency and statistical reliability.

Molecular Docking Study

The target protein structure was retrieved from the RCSB Protein Data Bank (https://www.rcsb.org/) for use in molecular docking studies. Prior to docking, the protein was prepared using the Protein Preparation Wizard, which involved steps such as optimization, minimization, and removal of water molecules and heteroatoms to ensure accurate binding site geometry.

Ligand molecules were also preprocessed using AutoDock Tools, where they were converted to the appropriate PDB format and optimized for docking by assigning torsions and calculating Gasteiger charges. A grid box was defined to encompass the active site residues of the target protein, ensuring precise docking within the functional region of the binding pocket.

The docking process was executed using PyRx software, employing the AutoDock Vina algorithm to predict binding conformations and affinities. Glide scores (binding affinities) were calculated to evaluate ligand–protein interactions. Post-docking analysis was conducted using Discovery Studio Visualizer, which facilitated identification of binding site residues and interaction types. Additionally, Maestro Visualizer was employed for detailed 3D rendering and structural interpretation of the docked complexes.

RESULTS AND DISCUSSION

The synthetic route comprised a two-step strategy. In the initial step, compounds 1 and 2 were subjected to cyclization in dioxane at 100 °C in the presence of $Pd_2(dba)_3$, Xantphos ligand, and cesium carbonate (Cs_2CO_3) as a base, leading to the formation of the quinazolinidione intermediate (A). The intermediate was subsequently purified by column chromatography.

In the second step, the purified intermediate A was coupled with a series of substituted anilines via amide bond formation, using T3P (propylphosphonic anhydride) as the coupling agent and triethylamine (TEA) as a base in dichloromethane (DCM) at room temperature. This step yielded the final amide derivatives B1–B5.

The chemical structures of the synthesized compounds were confirmed through ^1H NMR spectroscopy and LCMS analysis. The results of elemental analysis (C, H, N) were consistent with the calculated values, thereby validating the identity and purity of the synthesized derivatives.

Journal of Chemical Health Risks

www.jchr.org

JCHR (2025) 15(3), 2586-2592 | ISSN:2251-6727

***In vitro* Cancer Activity**

Table 4: *In vitro* anticancer activity of Compound

Compound	IC_{50} (µg/ml)
	MCF7
B1	12.4
B2	22.2
B3	9.1
B4	22.6
B5	10.2
Doxorubicin	1.0
Erlotinib	1.6

The cytotoxic potential of the synthesized quinazolinidione–amide derivatives (B1–B5) was evaluated against the MCF-7 human breast cancer cell line using the SRB assay. The IC_{50} values, representing the concentration required to inhibit 50% of cell proliferation, were calculated and compared with standard anticancer agents Doxorubicin and Erlotinib.

The results are summarized in Table 4. Among the synthesized compounds, B3 exhibited the highest cytotoxic activity with an IC_{50} of 9.1 µg/mL, followed by B5 (10.2 µg/mL) and B1 (12.4 µg/mL). Compounds B2 and B4 were comparatively less potent, with IC_{50} values of 22.2 µg/mL and 22.6 µg/mL, respectively.

As expected, the reference drugs Doxorubicin and Erlotinib showed significantly lower IC_{50} values of 1.0 µg/mL and 1.6 µg/mL, respectively, confirming their high cytotoxic efficacy.

Molecular Docking Study

The docking study compared the binding interactions and affinities of the synthesized compounds B1–B5 with those of reference drugs Erlotinib and Doxorubicin against a target protein. Compounds B1, B3, and B5 exhibited similar hydrophobic interactions with key residues including ALA719, LEU694, LEU764, LEU820, MET742, PHE699, and VAL702. In contrast, B2 and B4 demonstrated additional interactions with LEU768, indicating a slightly expanded hydrophobic binding profile.

All five synthesized ligands consistently formed hydrogen bonds with ASP831, CYS773, and MET769, suggesting a common polar interaction pattern. The calculated binding affinities revealed a range from –9.5 kcal/mol (B4) to –9.9 kcal/mol (B5), identifying B5 as the most potent binder, followed by B3 (–9.8 kcal/mol) and B1 (–9.7 kcal/mol).

In comparison, Erlotinib interacted hydrophobically with ALA719, ILE720, LEU694, LEU820, MET742, PHE699, and VAL702, and formed H-bonds with THR766, in addition to ASP831, CYS773, and MET769. However, its binding affinity was notably lower at –7.5 kcal/mol, indicating comparatively weaker binding strength.

Doxorubicin shared the hydrophobic interaction profile of B1, B3, and B5 but engaged in fewer hydrogen bonds—only with ASP831 and MET769—and exhibited a binding affinity of –9.6 kcal/mol, equal to B2 and slightly lower than B1–B5.

Overall, the B-series compounds demonstrated superior binding affinity compared to Erlotinib, with B5 emerging as the most promising ligand. The shared interaction patterns across the series suggest a conserved binding mode, with minor variations in hydrophobic contacts contributing to differences in binding strength. Erlotinib's distinct interaction with THR766 may reflect a divergent binding conformation, potentially explaining its reduced affinity.

Table 4: Molecular Docking Study Results of compounds B1-B5 with PDB Id: 1m17

Ligand	Binding Affinity kJ/mol
B1	-9.7
B2	-9.6
B3	-9.8
B4	-9.5
B5	-9.9
Erlotinib	-7.5
Doxorubicin	-9.6

Journal of Chemical Health Risks

www.jchr.org

JCHR (2025) 15(3), 2586-2592 | ISSN:2251-6727

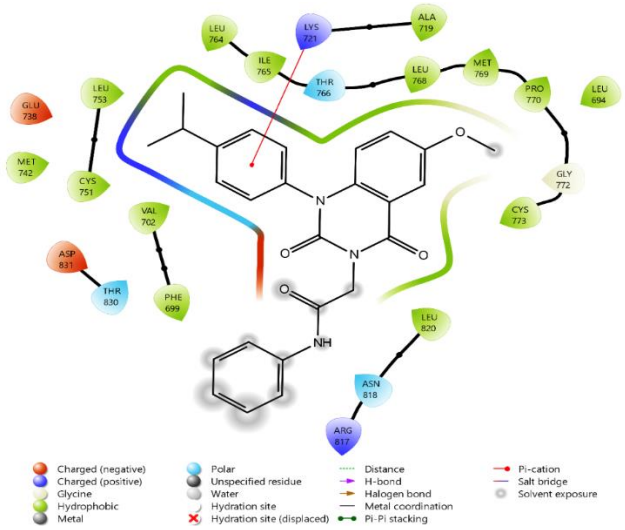

B1

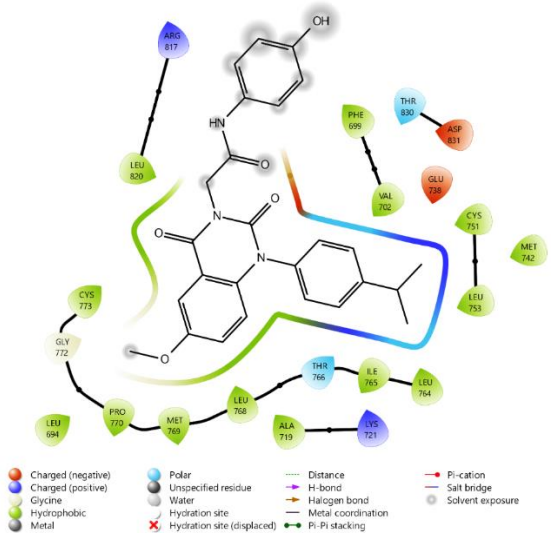

B4

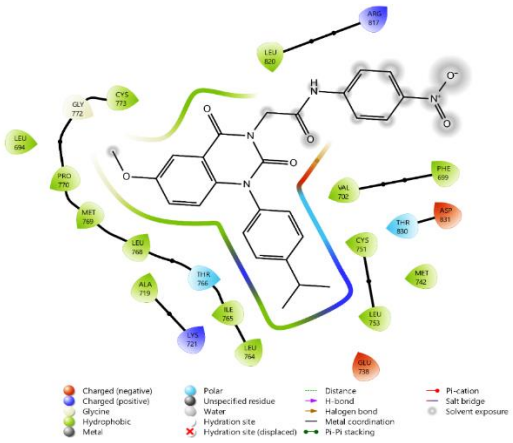

B2

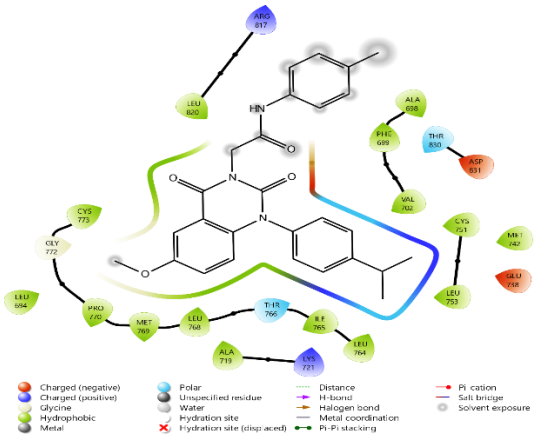

B5

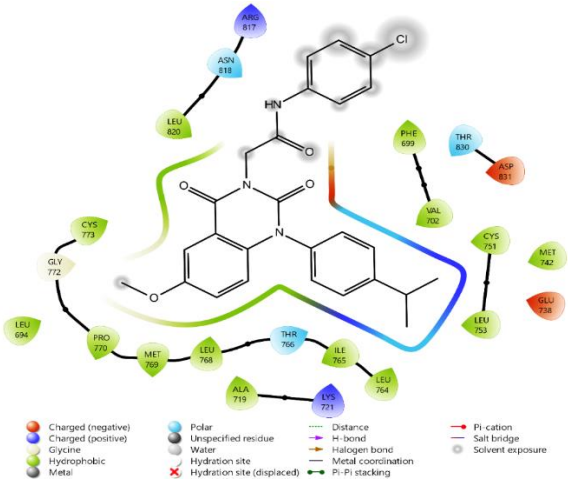

B3

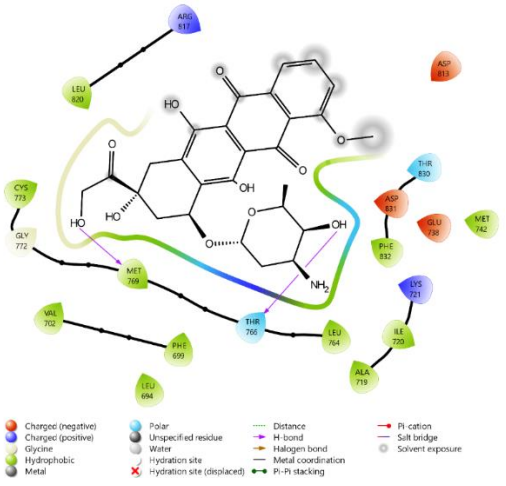

Doxorubicin

Journal of Chemical Health Risks

www.jchr.org

JCHR (2025) 15(3), 2586-2592 | ISSN:2251-6727

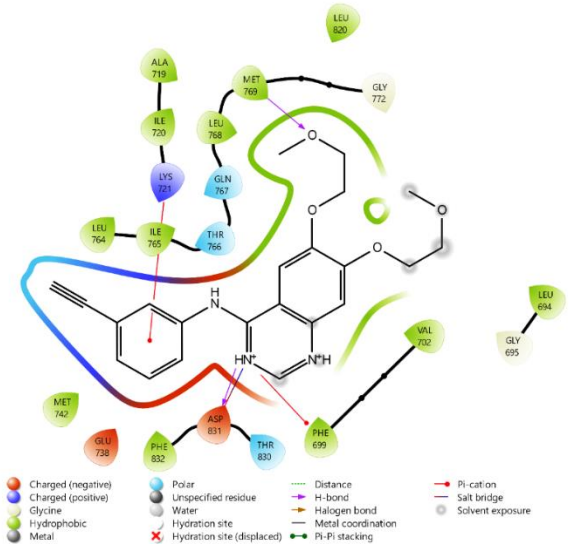

Erlotinib

Figure 1: Binding interactions of Compounds (B1-B5), Doxorubicin and erlotinib with PDB id: 1m17

These results suggest that the 5-series ligands, particularly B5, could be more effective binders than Erlotinib, though further stability validation would be necessary to confirm their potential as drug candidates.

CONCLUSION

In the present study, a novel series of quinazolinidione–amide derivatives (B1–B5) was successfully synthesized through a two-step protocol involving palladium-catalyzed cyclization and subsequent amide coupling with substituted anilines. Structural elucidation was accomplished using spectroscopic techniques such as ^{1}H NMR and LCMS, with elemental analysis confirming the purity of the synthesized compounds. The in vitro anticancer activity of these derivatives was evaluated against the MCF-7 breast cancer cell line using the SRB assay. Among the tested compounds, B3 and B5 demonstrated the most potent cytotoxic effects, with IC_{50} values of 9.1 µg/mL and 10.2 µg/mL, respectively, indicating promising antiproliferative potential. Molecular docking studies further supported these findings, revealing strong binding affinities and favorable interactions with key active site residues of the target protein. Notably, compound B5 exhibited the highest docking score (–9.9 kcal/mol), suggesting a strong and stable interaction profile. Overall, the combined biological and computational data highlight compounds B3 and B5 as promising lead molecules for further investigation and development as potential anticancer agents. Future studies involving detailed mechanistic evaluation and in vivo validation are warranted to advance these compounds in the drug discovery pipeline.

REFERENCES

[1]. Bidhendi SA, El Bialy SA. Quinazolinones as potential anticancer agents: advances in synthesis and biological activity. Curr Pharm Des. 2018;24(12):1234–45.

[2]. Fan Y, Zhang F, Xiong L, et al. Design, synthesis, and biological evaluation of 6-(imidazo[1,2-a]pyridin-6-yl)quinazolin-4(3H)-one derivatives as potent anticancer agents. Bioorg Chem. 2023;135:106484. doi:10.1016/j.bioorg.2023.106484

[3]. Trott O, Olson AJ. AutoDock Vina: improving the speed and accuracy of docking with a new scoring function, efficient optimization, and multithreading. J Comput Chem. 2010;31(2):455–61. doi:10.1002/jcc.21334

[4]. Forli S, Huey R, Pique ME, et al. Computational protein–ligand docking and virtual drug screening with the AutoDock suite. Nat Protoc. 2016;11(5):905–19. doi:10.1038/nprot.2016.051

[5]. Dhuguru J, Ghoneim OA. Quinazoline based HDAC dual inhibitors as potential anti-cancer agents. Molecules. 2022;27(7):2294. doi:10.3390/molecules27072294

[6]. Tawfik SS, Hamdi A, Ali AR, et al. S-alkylated quinazolin-4(3H)-ones as dual EGFR/VEGFR-2 kinase inhibitors: design, synthesis, anticancer evaluation and docking study. RSC Adv. 2024;14(36):26325–39. doi:10.1039/D4RA04828H

[7]. Huang J, Wang X, Dong R, et al. Discovery of N-(4-(3-isopropyl-2-methyl-2H-indazol-5-yl)pyrimidin-2-yl)-4-(4-methylpiperazin-1-yl)quinazolin-7-amine as a novel, potent, and oral cyclin-dependent kinase inhibitor. J Med Chem. 2021;64(17):12548–71. doi:10.1021/acs.jmedchem.1c00271

[8]. Mortazavi M, et al. Quinazoline-1,2,3-triazole hybrids as anticancer agents. Sci Rep.

Journal of Chemical Health Risks

www.jchr.org

JCHR (2025) 15(3), 2586-2592 | ISSN:2251-6727

2023;13:5432. doi:10.1038/s41598-023-32844-6

[9]. Al-Karmalawy AA, et al. Quinazolinone derivatives as potential anticancer agents: synthesis and biological studies. Biomolecules. 2022;12(4):456. doi:10.3390/biom12040456

[10]. Augustine A, Atta-ur-Rahman M. Applications of propylphosphonic anhydride (T3P) in peptide synthesis and green chemistry. Org Process Res Dev. 2009;13(5):945–53. doi:10.1021/op9001013

[11]. Hiebl J, et al. Large-scale synthesis featuring T3P amidations. J Pept Res. 1999;53(1):45–50. doi:10.1034/j.1399-3011.1999.530105.x

[12]. Al-Attas MS, et al. T3P®-mediated green amide coupling at room temperature. Tetrahedron Lett. 2015;56(22):3050–3. doi:10.1016/j.tetlet.2015.05.028

[13]. Sotriffer CA, Matter H. Scoring functions in protein–ligand docking. Curr Protein Pept Sci. 2007;8(5):373–85. doi:10.2174/138920307783220899

[14]. Eberhardt J, Santos-Martins D, Tillack AF, Forli S. AutoDock Vina 1.2.0: new docking methods, expanded force field, and Python bindings. J Chem Inf Model. 2021;61(8):3891–8. doi:10.1021/acs.jcim.1c00203

[15]. Sotriffer CA, Matter H. Protein–ligand docking: current status and future challenges. Protein Sci. 2006;15(5):984–95. doi:10.1110/ps.051843406